MicroRNA-92 modulates K(+) Cl(−) co-transporter KCC2 expression in cerebellar granule neurons

Christian Barbato,*,†,[1] Francesca Ruberti,†,[1] Massimo Pieri,‡,§ Elisa Vilardo,† Manuela Costanzo,† Maria Teresa Ciotti,† Cristina Zona‡,§ and Carlo Cogoni*,¶

*EBRI – European Brain Research Institute – Fondazione EBRI – Rita Levi-Montalcini, Rome, Italy

†INMM – Istituto di Neurobiologia e Medicina Molecolare, CNR, Rome, Italy

‡Department of Neuroscience, University of Rome 'Tor Vergata', Rome, Italy

§Fondazione S. Lucia, I.R.C.C.S., Rome, Italy

¶Dipartimento di Biotecnologie Cellulari ed Ematologia, Università di Roma 'La Sapienza', Rome, Italy

Abstract

MicroRNAs have been associated to fine-tuning spatial and temporal control of gene expression during neuronal development. The neuronal Cl(−) extruding, K(+)Cl(−) co-transporter 2 (KCC2) is known to play an important role in neuronal Cl(−) homeostasis and in determining the physiological response to activation of anion selective GABA receptors. Here we show that microRNA-92 is developmentally down-regulated during maturation of rat cerebellar granule neurons (CGNs) *in vitro*. Computational predictions suggest several high-ranking targets for microRNA-92 including the *KCC2* gene. Consistently, the KCC2 protein levels were up-regulated in mature CGN *in vitro* and a functional association between microRNA-92 and KCC2 3′ untranslated region was established using luciferase assays. The generation of an inward directed Cl(−) electrochemical gradient, necessary for the hyperpolarizing effect of GABA, requires robust KCC2 expression in several neuronal types. Here we show that lentiviral-mediated microRNA-92 over-expression reduced KCC2 protein levels and positively shifted reversal potential of GABA induced Cl(−) currents in CGNs. In addition KCC2 re-expression reversed microRNA-92 electrophysiological phenotype. Consistently microRNA-92 inhibition induced both an increase of the level of KCC2 and a negative shift in GABA reversal potential. These findings introduce a new player in the developmental change of GABA from depolarization to hyperpolarization.

Keywords: cerebellar granule neurons, development, GABA, KCC2, microRNA.

J. Neurochem. (2010) 113, 591–600.

MicroRNAs (miRNAs) are evolutionarily conserved, non-coding RNA molecules 18- to 25-nucleotides in length that post-transcriptionally regulate gene expression (Bartel 2004). In animals, miRNAs exert their function through base paring with the 3′ untranslated region (3′UTR) of specific target mRNAs, inducing either cleavage or translational repression of those mRNAs (Yekta *et al.* 2004). Although miRNAs may contribute in the regulatory gene networks in a number of biological processes, a prominent role of miRNAs is to regulate gene expression during development (reviewed in Bartel 2009). MiRNAs have been shown to be particularly abundant in the brain (Lagos-Quintana *et al.* 2002), where they were found to play a role in neuronal development, from early neurogenesis and cell-fate specification to neuronal differentiation (Kosik 2006; Barbato *et al.* 2008; Schratt 2009). Besides the miRNA function in neuronal specification and differentiation, the role of miRNA in post-mitotic neurons is less well characterized, although in the mature nervous system miRNAs are now emerging as key regulators of processes as synaptic plasticity (Ashraf and Kunes 2006).

Primary cultures of post-mitotic cerebellar granule neurons (CGNs), which are highly enriched for a single neuronal type, are one of the most widely used *in vitro* systems in neurobiology, providing a model for many aspects of neuronal development (Nakanishi and Okazawa 2006). CGNs develop over 7–10 days *in vitro* (DIV) and acquire some of the morphological, biochemical, and electrophysiological characteristics of mature neurons. In the present study, we used cultured CGNs to individuate miRNAs involved in neuronal maturation. We found that miR-92 is progressively down-regulated during CGNs *in vitro* development from 1 to 8 DIV. The neuron specific potassium K(+)- chloride Cl(−) co-transporter 2 (KCC2) was identified by first using the available prediction programs and then validated as a target of miR-92. KCC2 is known to play an important role in neuronal Cl(−) homeostasis and in determining the physiological response to activation of anion selective GABA and glycine receptors (Blaesse *et al.* 2009). In this study we describe a novel molecular mechanism of developmental KCC2 regulation mediated by miR-92 and we found that miR-92 acts in the developmental shift of GABA from depolarization to hyperpolarization in CGNs.

Materials and methods

Ethics statement/animals
All animals' experiments in this study were performed using Wistar rats that were housed in standard cages under a 12-h light-dark schedule at a constant temperature of 21°C with food and water *ad libitum*. All procedures involving rats were completed in accordance with the Istituto Superiore di Sanità (Italian Ministry of Health) and current European (directive 86/609/ECC) Ethical Committee guidelines.

miRNA northern blotting
To obtain differential expression profile of miR-92 from 1, 4 and 8 DIV cultured CGNs, total RNA was extracted using Trizol and analysed by northern blotting. RNA (30 μg) from CGN$_S$ was run out on Tris Borate/EDTA 10% Acrylamide-7M urea denaturing gels, and transferred to XL Hybond membrane (GE Healthcare, Milano, Italy), cross-linked and hybridized with specific DNA probes corresponding to U6 snRNA or miRNA-92 radiolabeled using [-α^{32}P]ATP (6000 Ci/mmol) by DNA polymerase primer extension. In particular tailed DNA probes were synthesized with the following oligonucleotides: universal template TTTTTTTTTTggatgg; U6 probe: AGTATATGTGCTGCCGAAGCccatcc; miR-124 probe: GGCATTC-ACCGCGTGCCTTAccatcc; miR-92 probe: CAGGCC GGGACAAGTGCAAT-Accatcc using Klenow fragment DNA polymerase 3′-5′-exo- (New England Biolabs, Ipsiwich, MA, USA).

Neuronal cultures
Cultures enriched in granule neurons were obtained from dissociated cerebella of 8-day-old Wistar rats. Cells were plated in basal medium Eagle supplemented with 10% heat-inactivated fetal bovine serum, 25 mM KCl, 2 mM glutamine (Life Technologies, Monza, Italy) and 100 μM gentamicin sulfate, on dishes (Nunc, EuroClone, Milano, Italy) coated with poly-L-lysine. Cells were plated at 2.5×10^6 per 35 mm dish. 1β-Arabinofuranosylcytosine (10 mM) was added to the culture medium 18–22 h after plating to prevent proliferation of non-neuronal cells. Rat PC12 cells were cultured in RPMI 1640 medium with 5% fetal bovine serum and 10% heat-inactivated horse serum in a 5% CO_2-humidified incubator at 37°C.

Transient transfection of cerebellar granule neurons at 4 DIV (using 0.8 μg of either KCC2-IRES-Tomato (internal ribosome entry site) (Bortone and Polleux 2009) or IRES-Tomato per 24 well) was performed using Ca-phosphate transfection method (Ruberti and Dotti 2000).

IRES-Tomato was derived from KCC2-IRES-Tomato: hKCC2 was excised by *Xho*I restriction enzyme and vector backbone was gel purified and riligated.

Luciferase reporter gene constructs and luciferase assay
The KCC2 3′UTR (SG-Luc-SLC12A5; Amplicon start: chr20: 44119626; Amplicon end: chr20: 44122225) was purchased from Switch Gear Genomic (Menlo Park, CA, USA). The SG control firefly luciferase no containing 3′UTR was derived from SG-Luc-SLC12A5. PC12 cells were plated the day before transfection 3×10^5 per well in 24-well plates. The following day 50 pmoles of miRNA duplexes (Dharmacon EuroClone, Milano, Italy), 30 ng of firefly luciferase expression vectors and 15 ng of renilla luciferase expression vector (pRL-TK; Promega Italia, Milano, Italy) were co-transfected into the cells using 1.2 μL of Lipofectamine 2000 (Invitrogen, San Giuliano Milanese, Italy). Cells were lysed 24 h after transfection, and lucifease assays were performed using the Dual Luciferase Reporter Assay System (Promega) according to the manufacture's protocols. The experiments were carried out in triplicate.

miRNA and miRNA sponge lentiviral vectors and viral particles preparations
The following oligonucleotides: 92a up: TGCAGGCCGGGACAA-GTGC-AATACTCGAGTATTGCACTTGTCCCGGCCTGCTTTT-TC; 92a down: TCGAGAAAAAGCAGGCCGGGACAAGTG-CAATACTCGAGTATTGCACTTGTCCCGGCCTGCA containing the mature miR-92a sequence in an artificial stem loop were designed and cloned into the pLB lentiviral vector (Addgene plasmid 11619) (Kissler *et al.* 2006) using the *Hpa*I and *Xho*I restriction sites.

In order to produce a sponge backbone the cytomegalovirus (CMV) promoter, which drives green fluorescent protein (GFP) expression in pLB, was replaced by *Age*I/*Not*I excision and introduction of the human synapsin 1 promoter (470 bp) within the *Xba*I/*Eco*RI fragment excised from pHSYN-MH4-I (Kuegler *et al.* 2001). Incompatible cohesive end were blunt ended with Klenow DNA polymerase and by cloning a lentiviral plasmid with the synapsin promoter (pLSyn) was produced.

Using the following oligonucleotides S1 CATAACAGGCCGGG AACGTGCAATACGATCAGGCCGGGAACGTGCAATAACCGGT; AS1 TATTGCACGTTCCCGGCCTGATCGTATTGCACGTTCCCG GCCTGTTATGGTAC; S2 CAGGCCGGGAACGTGCAATATCACC AGGCCGGGAACGTG CAATACCCGGGGGTACCGAGCT; AS2 CGGTACCCCCGGGTATTGCACGTTCCCGGCCTGGTGATATTG-CACGTTCCCGGCCTGACCGGT; miR-92 sponge was constructed. In particular oligonucleotides S1 and S2 containing four tandem bulged (at position 9–11) miR-92 binding sites were annealed with AS1 and AS2 respectively, ligated, digested with *Kpn*I restriction enzyme, purified and

cloned into the *Kpn*I site of pLSyn backbone downstream of woodchuck hepatitis virus post-transcriptional regulatory element.

The G glycoprotein vesicular stomatitis virus-pseudotyped lentiviral particles were generated by Fugene HD (Roche, Monza, Italy) transfection of HEK293T cells with a mixture of either pLB or pLSyn lentiviral vector and three plasmids (kindly provided by L. Naldini) (Dull *et al.* 1998) that are essential to produce third-generation lentiviruses. Cells were cultured in Dulbecco's modified Eagle's medium (DMEM) supplemented with 10% fetal bovine serum, 100 U/mL penicillin G, and 100 μg/mL streptomycin at 37°C in 5% CO_2. Cells were plated at 1.8×10^6 cells in a 10-cm dish 24 h before transfection. Fifteen hours after incubation with the transfection mix at 37°C, the cells were washed with DMEM, and complete DMEM was added. Virus-containing medium was harvested 60 h after transfection, filtered through a 0.45-μm Durapore Stericup unit, and concentrated by one ultracentrifugation step.

Western blot analysis

Equal amounts of proteins were separated by 7% sodium dodecyl sulfate–polyacrylamide gel electrophoresis. After blotting on nitrocellulose membrane (Hybond ECL, GE Healthcare), the proteins were visualized using appropriate primary antibodies. All primary antibodies were diluted in 5% (w/v) non-fat dry milk Tris Buffered Saline 1× and incubated with the nitrocellulose blot overnight at 4°C. Incubation with secondary peroxidase-coupled anti-mouse or anti-rabbit antibodies was performed at 21°C for 45 min. Immunoreactivity was detected by chemiluminescence visualization. The following antibodies have been used: rabbit polyclonal anti-KCC2 (1 : 1000) (Millipore, Milano, Italy) mouse monoclonal anti-Glyceraldehyde 3-phosphate dehydrogenase (GAPDH) (1 : 6000) (Covance, Princeton, New York, NY, USA).

Electrophysiological recording

Cultured granule cells grown for 8 DIV were voltage clamped at various holding potentials using the perforated patch-clamp technique (Akaike 1996) on the stage of an inverted fluorescence microscope (Carl Zeiss, Arese, Milano, Italy) at 21°C. Borosilicate glass patch pipettes with a resistance in the bath of 3–4 MΩ were made with a PP 83 puller (Narishige, Tokyo, Japan) and filled with a solution containing (in mM): 125 KCl, 1.2 MgCl$_2$, 10 HEPES, 1 EGTA, 2 ATP-Na$_2$, pH 7.3 with KOH. Gramicidin (Sigma-Aldrich, Milano, Italy) was dissolved in dimethylsulfoxide (50 mg/mL). Before filling the electrode with Gramicidin-containing solution (50 μg/mL), the tip of the electrode was always loaded with a small volume of antibiotic-free electrode solution in order to avoid interference of the antibiotic with seal formation (Kyrozis and Reichling 1995). After seal formation, access resistance was monitored until it reached a stable value (< 30 MΩ). Cells were bathed in a solution containing (in mM): 130 NaCl, 5.9 KCl, 3.2 CaCl$_2$, 1.2 MgCl$_2$, 11.6 HEPES, 11.5 glucose, pH 7.4 with NaOH. Tetrodotoxin (1 μM; Alomone Labs, Jerusalem, Israel), cadmium (100 μM, Sigma-Aldrich) and D-2-amino-5-phosphonovaleric acid (AP5, 10 μm; Sigma-Aldrich) were added to the external solution to block voltage-gated Na$^+$ and Ca^{2+} channels and NMDA receptors, respectively. The culture dish in the recording chamber was continuously perfused (1 mL/min) with the bath solution. GABA (water stock solution of 50 mM; Sigma-Aldrich) was dissolved in the bath solution and applied directly with a fast multibarrel pipette perfusion system controlled by electronic valves (SF-77B Perfusion fast step, Warner Instrument, Hamden, CT, USA) placed within 100 μm of the recorded cell. Currents were monitored with an Axoclamp 200B patch amplifier (Axon Instrument, Foster City, CA, USA), filtered at 2 kHz, sampled at 50 kHz and digitized in a computer with pClamp9 software (Axon Instrument) for off-line analysis. The reversal potential for I$_{GABA}$ was determined measuring current voltage relationships during GABA pulses application and used to estimate the intracellular chloride concentration [Cl$^-$]$_i$ based on the Nernst equation for Cl$^-$. To ensure that the gramicidin-perforated patch clamp mode was done properly, the reversal potential for I$_{GABA}$ was also calculated under the whole-cell configuration of the patch-clamp technique by application of negative pressure through the recording pipette and compared with the value calculated by Nernst equation.

Results are expressed as mean ± SD. Statistical analysis was performed using an unpaired *t*-test or one-way ANOVA followed by Bonferroni's test for multiple comparisons when necessary; values were considered significantly different for a $p < 0.05$ (Origin 6.1, MicroCal Software, Northampton, MA, USA).

Results

Anti–parallel expression of miRNA–92 and its putative target KCC2, during CGNs development

To investigate the roles of miRNAs in the regulation of development and maturation processes in CGNs, we profiled the miRNAs expression pattern at 4 DIV and 8 DIV cultured CGNs using microarray. Few significative miRNAs were found to be differentially expressed during the two CGNs developmental time-points, among them the miR-92 was found to be down-regulated > 2-fold from 4 DIV to 8 DIV (data not shown). Northern blot analysis confirmed that the miR-92 expression level progressively declines during CGNs development from 1 DIV to 8 DIV (Fig. 1a and b). As expected miR-124 expression was significantly up-regulated during CGNs maturation (Fig. 1a). Consistently, we found that miR-92 also decreased during postnatal development of rat cerebellum from P3 to P21, at which time CGNs are completely differentiated (Fig. 1c).

In order to identify putative miR-92 target mRNAs we used several miRNA target prediction programs available on the web, which use miRNAs-mRNA sequence complementarity and miRNAs-mRNA duplex thermodynamics, as TargetScan (Lewis *et al.* 2005), Pictar (Krek *et al.* 2005) and miRanda (Griffiths-Jones 2006). All the algorithms identify the neuronal specific gene *Slc12a5*, alias *KCC2,* as a high score miRNA-92 target, predicting either two or four putative miR-92 responsive elements (REs) in the KCC2 3′UTR (Fig. 2a). As second step, we employed MicroRNA Database (Wang and El Naqa 2008) which uses a machine learning approach, extracting relevant information from data automatically throughout computational and statistical methods. MicroRNA Database also predicts that *KCC2* gene is a miR-92 target with the top higher prediction score of 99/100.
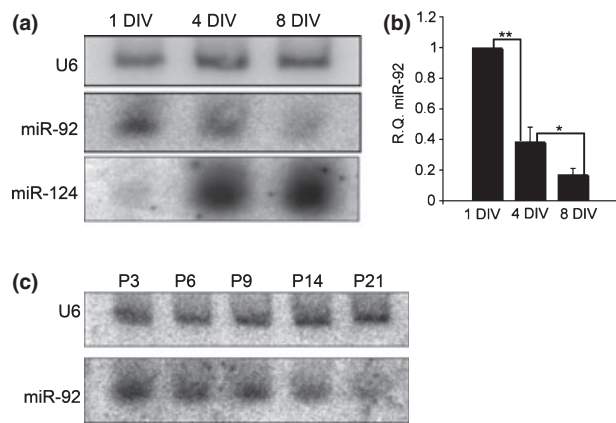
Fig. 1 miR-92 down-regulation in rat CGNs during *in vitro* maturation and in developing rat cerebellum. (a) Northern blot analysis of mature miR-92 from total RNA of CGN cultures at different days *in vitro*. miR-124, as described in other neuronal systems, was expressed at higher level in mature neurons. (b) The intensity of the bands from three independent experiments was analysed quantitatively by densitometry and the results obtained with miR-92 probe were normalized with the U6 signal and plotted by Relative Quantification (RQ) method using 1 DIV CGNs as 1-fold. Results are expressed as mean ± SD. *$p < 0.05$; **$p < 0.01$ (*t*-test). (c) Northern blot of mature miR-92 in developing cerebellum from postnatal day 3 (P3) to 21 (P21). U6 RNA was used as loading control. These results are representative of two independent experiments.

KCC2 is a neuronal specific gene that has been shown to be expressed at high levels in post-mitotic neurons including rat CGNs (Mikawa *et al.* 2002). We analysed the expression of KCC2 protein at different development time-points in CGNs cultured *in vitro* and found that KCC2 protein level is low at beginning of the maturation (1 DIV) and progressively increases at 4 DIV reaching a high level at 8 DIV (Fig. 2b). Strikingly, there is an inverse correlation between miR-92 and KCC2 expression levels during the CGNs development. The anti-parallel regulation of miRNA and target mRNA has been frequently observed during cellular differentiation and has been proposed may constitute a kind of 'switch' able to ensure an additional level of gene regulation, increasing the robustness of the gene regulatory network (Bartel 2009).

miR–92 modulates KCC2 expression by interaction with the 3′UTR of KCC2 mRNA

In order to investigate the interaction between miR-92 and KCC2 3′UTR we used a firefly reporter vector containing downstream of the luciferase open reading frame the full length KCC2 3′UTR. Rat PC12 cells were transfected with a firefly construct containing the KCC2 3′UTR or a control firefly plasmid together with either a miR-92 precursor or a control miRNA. We observed that the full length KCC2 3′UTR in presence of miR-92 reduces significantly firefly luciferase activity, more than 70%, respect to the control (Fig. 3a). These data indicated that miR-92 represses KCC2 expression.

Fig. 2 KCC2 is a potential miR-92 target gene. (a) Table showing the sequence (bold) and location of the miR-92 REs predicted in the KCC2 3′ UTR by public-access miRNA target prediction databases. (b) Representative western blot of KCC2 in CGNs from early stage of growth (1 DIV) up to 8 DIV was shown. GAPDH was used as normalization control. (c) The intensity of the bands from three independent experiments was analysed quantitatively by densitometry and the results obtained with the anti-KCC2 antibody were normalized with the anti-GAPDH signal and plotted by Relative Quantification (RQ) method using 8 DIV CGNs as 1-fold. Results are expressed as mean ± SD.
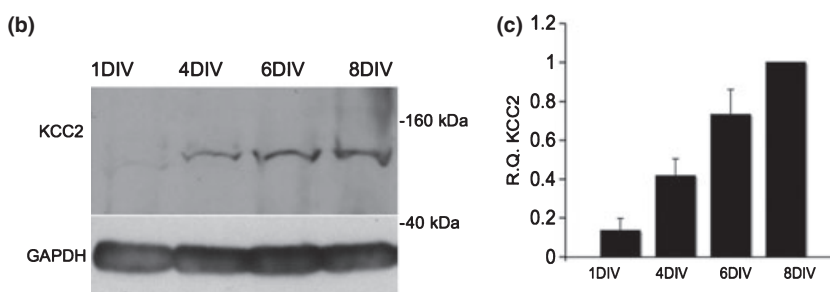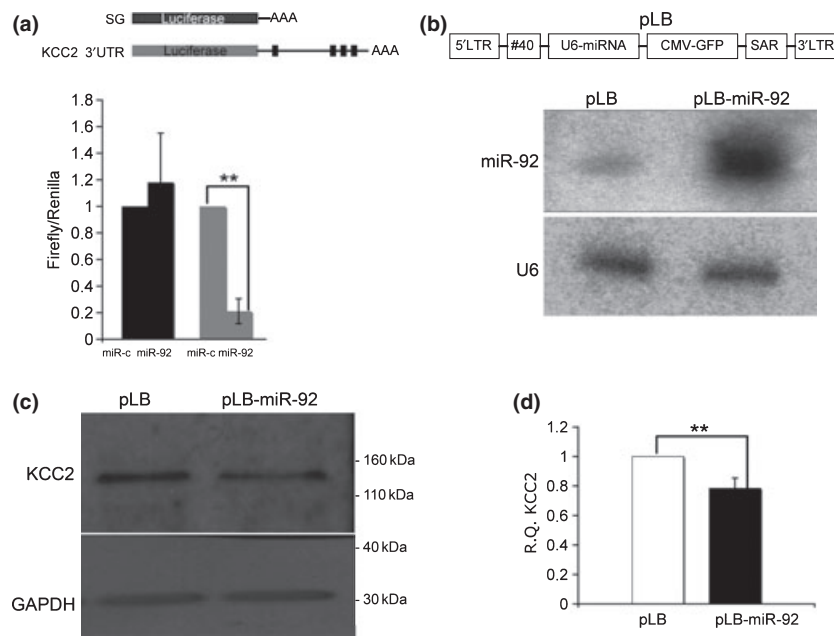
Fig. 3 Post-transcriptional regulation of KCC2 expression by miR-92. (a) Schematic representation of the firefly plasmids used in the dual luciferase assay performed in PC12 cells. Black boxes in the KCC2 3′UTR indicate miR-92 REs. PC12 cells were transfected independently with each one of the two luciferase reporter genes together with either miR-92 or control miRNA (miR-c) (50 nM). At 24 h after transfection, luciferase activity was determined and normalized to the Renilla control. Values were calculated by dividing the normalized activity of miR-92 transfected cells to that one of PC12 cells transfected with miR-c. Data represent the mean of three independent experiments ± SD. **$p < 0.01$ (t-test). (b), Scheme of pLB lentiviral vector that contains the anti-repressor element #40 and scaffold-attached region (SAR) that enhances general promoter function. The U6 and CMV promoters drive miRNA and GFP expression, respectively. *In vitro*

CGNs (1 DIV) were transduced either with replication defective lentivirus expressing miR-92 (pLB-miR-92) or with control lentivirus (pLB) and analysed at 8 DIV. Northern blot analysis of small RNAs (< 200 nt) isolated from CGNs. A 32P-labeled probe complementary to miR-92 was hybridized following a northern blot procedure for the detection of small RNAs. U6 RNA was probed as a control. (c) Protein extracts from CGNs were analysed by immunoblotting using an antibody recognizing KCC2 or an antibody against GAPDH and the immunoreactive bands were revealed by chemiluminescence visualization. (d) The intensity of the bands from three independent experiments was analysed quantitatively by densitometry and the results obtained with the anti-KCC2 antibody were normalized with the anti-GAPDH signal and plotted by RQ method using pLB CGNs as 1-fold. Results are expressed as mean ± SD. **$p < 0.01$ (t-test).

To address whether miR-92 may regulate endogenous KCC2 expression in CGNs, we over-expressed miR-92 in CGNs at 8 DIV, using a bicistronic lentiviral vector expressing GFP under the control of the cytomegalovirus promoter and in which the miR-92 sequence was inserted into an artificial hairpin structure under the control of U6 promoter (Fig. 3b). The over-expression of miR-92 was verified by northern blot analysis of small RNAs isolated from lentiviral miR-92 transduced CGNs and, as a control, from neurons transduced with a lentiviral control vector (Fig. 3b). By Western blot analysis, we found that miR-92 over-expression affects significantly KCC2 protein levels (Fig. 3c and d), supporting a role of miR-92 in the control of KCC2 expression during CGNs development.

MicroRNA–92 over-expression leads to a change in responsiveness to GABA which is reversed by KCC2 re-expression

In order to evaluate whether miR-92 over-expression produces functional effects on the level of intracellular

Cl(−), electrophysiological recording was performed on lentiviral transduced CGNs at 8 DIV. GFP positive granule cells were analyzed using perforated patch clamp recording. The resting membrane potential of neurons measured in current-clamp recordings was −60 ± 3.3 mV for pLB neurons ($n = 15$) and –58.7 ± 2.8 mV for pLB-miR-92 neurons ($n = 15$; $p > 0.05$). Reversal potential (E_{rev}) of GABA-induced Cl(−) currents in lentiviral transduced CGNs at 8 DIV, was measured in voltage-clamp mode. The GABA-induced Cl(−) currents were obtained by 10 µM GABA application at different holding potential recorded from pLB and pLB-miR-92 CGNs (Fig. 4a). E_{rev} of GABA-induced Cl(−) currents was calculated by a linear regression fit of the current-voltage relationship (Fig. 4b). The analysis of population data showed that E_{rev} for GABA was positively shifted in CGNs over-expressing miR-92 (−46.6 ± 9.8 mV, $n = 15$) relative to control pLB transduced neurons (−60.3 ± 6.3 mV, $n = 15$) (Fig. 4c) (t-test $p < 0.001$). Measurements of intracellular Cl(−)in pLB and pLB-miR-92-expressing neurons were derived by Nerst equation. Compared with
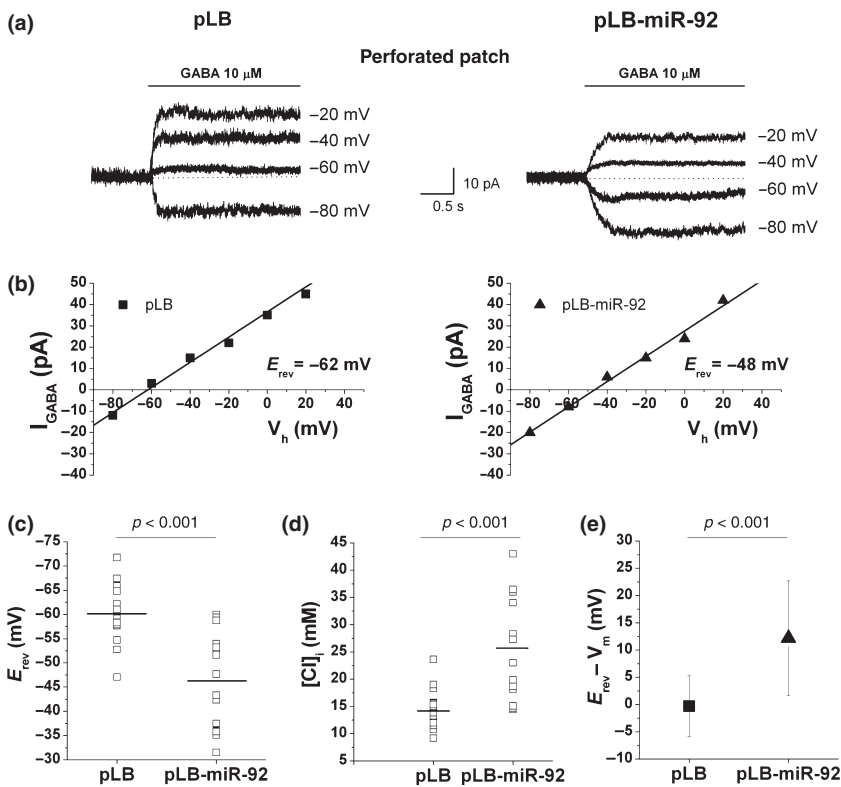
Fig. 4 Cerebellar granule cell E_{rev} for GABA shifts to more positive values in miR-92 over-expressing neurons. (a) Representative current recordings elicited by 10 μM GABA at different holding potential recorded in pLB and pLB-miR-92 CGNs in the gramicidin-perforated patch condition. (b) Current-voltage relationship of the GABA-induced currents from the neurons shown in (a). E_{rev} was −62 mV in pLB cell and −48 mV in pLB-miR-92. (c) Scatter plot of E_{rev} for pLB and pLB-miR-92 cells. The mean values for E_{rev} (bar) were −60.3 + 6.3 mV (n = 15) for pLB cell and −46.6 + 9.8 mV (n = 15) for pLB-miR-92 (p < 0.001). (d) Scatter plot of intracellular chloride $[Cl^-]_i$ calculated using Nernst equation. The $[Cl^-]_i$ mean values (bar) for pLB-miR-92 and pLB were significantly different (p < 0.001). (e) Means and SD of the driving force of pLB (n = 15) and pLB-miR-92 (n = 15) neurons. The mean values of pLB-miR-92 cells are significantly different compared to control cells (p < 0.001).

control cells, miR-92 over-expression resulted in higher level of intracellular Cl(−) (25.6 ± 9.5 mM in miR-92 over-expressing cells; 14.6 ± 3.7 mM in control neurons; *t*-test p < 0.001) (Fig. 4d). In addition, the driving force ($E_{rev} - V_m$) values in CGNs over-expressing miR-92 were significantly higher (12.2 ± 10.5 mV) compared to control neurons (−0.3 ± 5.6 mV; p < 0.001; Fig. 4e), indicating that GABA receptors, when activated in neurons over-expressing miR-92, have a more depolarizing effect. It should be noted that miR-92 over-expression modified heavily the E_{rev} of GABA (Fig. 4c) while induced a small reduction in KCC2 protein levels as reported by western blot analysis (Fig. 3c and d). This discrepancy can be partially explained by the fact that electrophysiological recording was performed only on lentiviral transduced neurons while western blot analysis included also granule neurons which are not expressing exogenous miR-92. Indeed to avoid lentiviral toxicity less than 100% CGNs were transduced.

In order to establish whether the electrophysiological phenotype recorded in pLB-miR-92 granule cells was mediated by KCC2 reduction, pLB-miR-92 transduced CGNs at 4 DIV were transfected with human KCC2-IRES-Tomato expression plasmid (Bortone and Polleux 2009). Reversal potential of GABA induced Cl(−) currents in GFP/Tomato double positive granule cells at 8 DIV was measured (Fig. 5a). The analysis of population data showed that the E_{rev} mean for GABA induced currents was negatively shifted in CGNs over-expressing miR-92 and re-expressing KCC2 (−67.0 ± 10.2 mV, n = 13) compared with GFP positive cells only over-expressing miR-92 (−47.8 ± 9.1 mV, n = 8; Bonferroni test, p < 0.001). In particular the mean E_{rev} values of miR-92 CGNs re-expressing KCC2 was similar to the mean values obtained by control granule cells at 8 DIV transduced with pLB lentivirus and transfected with control IRES-Tomato expression vector (−61.5 ± 9.8 mV, n = 8) (Fig. 5b). Moreover pLB-miR-92 positive neurons, re-expressing KCC2, resulted in lower intracellular chloride concentration (11.9 ± 9.1 mM; n = 13; Bonferroni test, p < 0.001) and lower driving force (−10.5 ± 17.4 mV; n = 13; Bonferroni test, p < 0.01) compared to pLB-miR-92 neurons (24.1 ± 7.6 mM for $[Cl^-]_i$; 10.3 ± 8.2 mV for the driving force; n = 8) these values were not significantly differents with pLB + Tomato neurons (14.5 ± 5.9 mM for $[Cl^-]_i$; −2.6 ± 5.1 mV for the driving force; n = 8) (Fig. 5c and d). We can conclude that KCC2 re-expression is able to reverse the effects of neuronal PLB-miR-92 over-expression.

miR–92 inhibition by lentiviral sponge induces both increased KCC2 protein levels and a negative shift in GABA reversal potential

MicroRNA sponge expression constructs that carry miRNA recognition motifs in their 3′ UTR have been found to bind and titer miRNAs and thus inhibit miRNA functions (Ebert *et al.* 2007; Gentner *et al.* 2009). In order to evaluate whether endogenous miR-92 regulates KCC2 protein abundance in
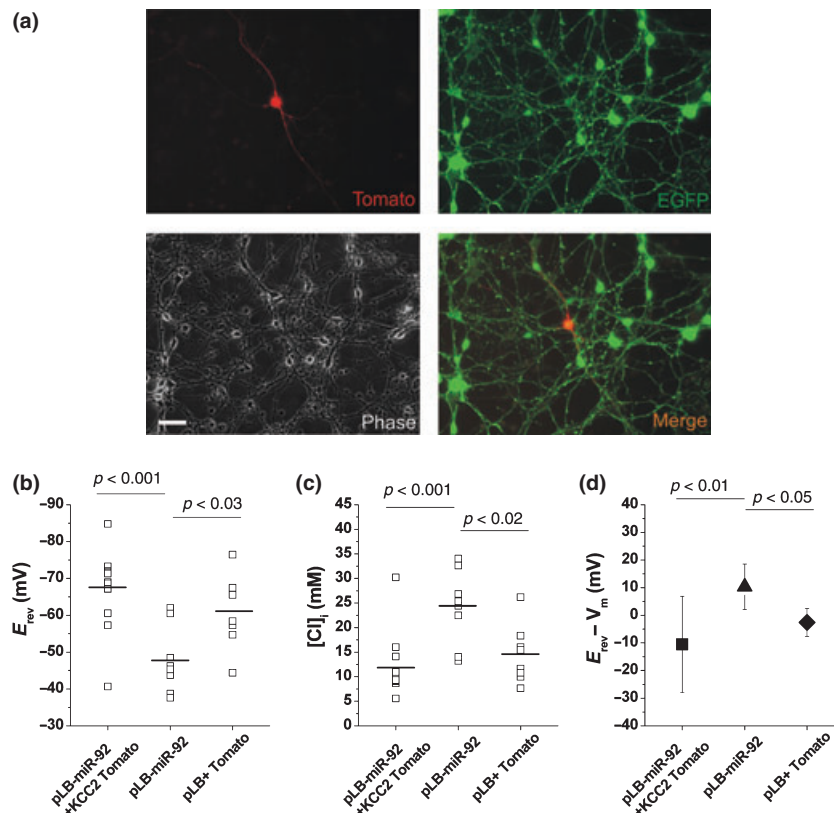
Fig. 5 KCC2 re-expression reverses miR-92 electrophysiological phenotype. (a) CGN at 8 DIV transduced with pLB-miR-92 expressing GFP and transfected with hKCC2-IRES-Tomato. Electrophysiological recording was performed either on GFP positive cells or on GFP/Tomato merged double positive cells. A phase contrast of the same field showed the morphology of healthy neurons (scale bar = 12 μm). (b) Scatter plot of E_{rev} for pLB-miR-92 + KCC2, pLB-miR-92 and pLB + Tomato cells. The mean values for E_{rev} (bar) were -67.0 ± 10.2 mV ($n = 13$) for pLB-miR-92 + KCC2; -47.8 ± 9.1 mV ($n = 8$) for pLB-miR-92 and -61.5 ± 9.8 mV ($n = 8$) for pLB + Tomato cells (Bonferroni test). (c) Scatter plot of intracellular chloride $[Cl^-]_i$ for pLB-miR-92 + KCC2, pLB-miR-92 and pLB + Tomato cells. The $[Cl^-]_i$ mean values (bar) for pLB-miR-92 (24.1 ± 7.6 mM) were significantly different respect to pLB-miR-92 + KCC2 (11.9 ± 6.0) and to pLB + Tomato (14.5 ± 5.9 mM) (Bonferroni test). (d) Means and SD of the driving force of pLB-miR-92 + KCC2 (-10.5 ± 17.4 mV; $n = 13$; ANOVA, $p < 0.01$ respect to pLB-miR-92), pLB-miR-92 (10.3 ± 8.2 mV; $n = 8$) and pLB + Tomato neurons (-2.6 ± 5.1 mV; $n = 8$).

granule cells we over-expressed a miR-92 sponge in CGNs using a lentiviral vector (pLSyn) in which the synapsin promoter controls expression of four tandem bulged miR-92 REs located downstream of the GFP open reading flame. By immunofluorescence analysis we found that, in CGNs transduced either with pLSyn or pLSyn-miR-92 sponge, GFP fluorescence increased between 4 and 8 days *in vitro* showing that synapsin promoter activity increases during CGN development (Fig. 6a). Lentiviral transduced CGN at 4 DIV expressed GFP mRNA at sub-saturating level such that allowed us to observe a strong reduction of GFP fluorescence in pLSyn-miR-92 sponge CGNs (Fig. 6a-ii) respect to pLSyn CGNs (Fig. 6a-i). This evidence indicated suppression of GFP translation by endogenous miR-92. Thereafter the functional effects of miR-92 sponge were assessed in CGN at 6 DIV, a time in which developing of CGNs is still occurring and synapsin promoter activity is sufficiently high. By Western blot analysis, we found that the miR-92 sponge increases significantly KCC2

protein levels (Fig. 6b and c), confirming a role of endogenous miR-92 in the control of KCC2 expression during CGNs development. We next asked whether the responses to GABA were affected by endogenous miR-92 inhibition. GFP positive granule cells were analyzed using perforated patch clamp recording. The resting membrane potential mean measured in current clamp perforated patch recordings was -56.9 ± 5.0 mV ($n = 10$) in pLSyn neurons and -57.1 ± 6.8 mV ($n = 9$) in pLSyn-miR-92 sponge neurons (t-test, $p > 0.05$). Reversal potential (E_{rev}) of GABA-induced Cl(−) currents (10 μM GABA application) in lentiviral transduced CGNs at 6 DIV, was measured in voltage-clamp mode by varying the holding potential of the cell (Fig. 7a). E_{rev} of GABA-induced Cl(−) currents was calculated by a linear regression fit of the current-voltage relationship (Fig. 7b). The analysis of population data showed that E_{rev} mean for GABA was negatively shifted in CGNs expressing pLSyn-miR-92 sponge (-61.3 ± 6.9 mV, $n = 9$) compared to control pLSyn transduced neurons
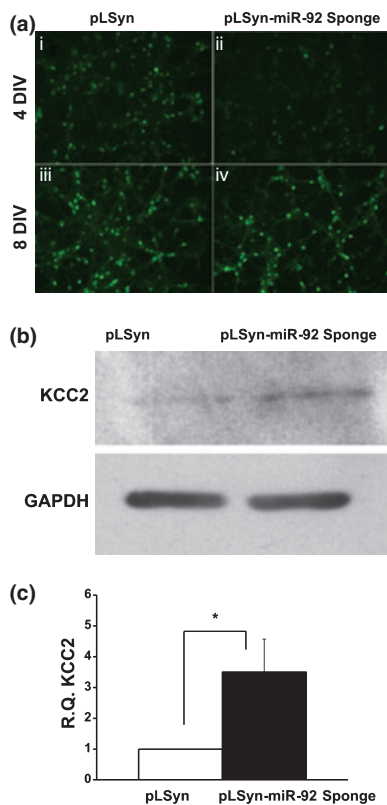
Fig. 6 miR-92 inhibition induces robust KCC2 expression. (a) In CGNs transduced either with pLSyn or pLSyn-miR-92 sponge GFP signal increases from 4 up to 8 DIV. In CGNs at 4 DIV GFP signal was visibly lower in pLSyn-miR-92 sponge neurons (b) relative to pLSyn neurons (a). Images were captured at 20× magnification. (b) Protein extracts from CGNs at 6 DIV were analysed by immunoblotting analysis using an antibody recognizing KCC2 or an antibody against GAPDH and the immunoreactive bands were revealed by chemiluminescence visualization. (c) The intensity of the bands from three independent experiments was analysed quantitatively by densitometry and the results obtained with the anti-KCC2 antibody were normalized with the anti-GAPDH signal and plotted by RQ method using pLSyn CGNs as 1-fold. Results are expressed as mean ± SD. *$p < 0.05$ (t-test).

(-51.6 ± 11.2 mV, $n = 10$; t-test, $p < 0.04$) (Fig. 7c). Measurements of intracellular Cl($-$) in pLSyn miR-92 sponge expressing neurons (14.1 ± 3.7 mM, $n = 9$) compared with control cells (21.6 ± 9.7 mM, $n = 10$; t-test $p < 0.05$) (Fig. 7d), resulted in lower level of intracellular Cl($-$). In addition, the driving force ($E_{rev} - V_m$) mean values in CGNs over-expressing miR-92 sponge (-4.4 ± 6.2 mV; $n = 9$) was significantly lower compared to control neurons (5.5 ± 7.3 mV, $n = 10$; t-test, $p < 0.001$); (Fig. 7e). We conclude that miR-92 regulates E_{rev} of GABA induced Cl($-$) currents in CGNs.

Discussion

The regulation of gene expression by miRNAs has been found particularly relevant, in dividing cells, for the control of cellular developmental processes. It has been frequently observed that, during development, when a microRNA is up-regulated often its target genes are concomitantly down-regulated or vice versa (Bartel 2009). This mechanism may serve either to stabilizes the commitment of a differentiating cell or for the fine-tuning of the target gene levels, in a timely regulated mode, during differentiation. In this study we show that gene regulation by miRNAs may also be significant in controlling gene expression in post-mitotic cells. We used cultures of post-mitotic primary CGNs from early postnatal rats and from preliminary microRNA micro-array analysis we found that miR-92 was significantly timely regulated during the maturation process of CGNs that occurs *in vitro*. Thus miR-92 is expressed at high level at 1 DIV CGN cultures and is progressively down-regulated at time points 4 and 8 DIV. The *KCC2* gene is predicted by several programs as the top high score target of miR-92. Four miR-92 REs are present in the 3′UTR of KCC2 mRNA and we demonstrated that KCC2 3′UTR mediates translational repression in luciferase reporter assays. Site directed muta-genesis studies of miR-92 RE in KCC2 3′UTR will be necessary to evaluate the contribution of each site to regulation of KCC2 expression. These experiments should allow us to establish the sites specifically involved in the regulation and to address whether they act in additive and/or synergistic fashion (Grimson *et al.* 2007).

KCC2 is a potassium K(+) chloride Cl($-$) co-transporter which is specifically expressed in neurons and abundant in the mature CNS (Blaesse *et al.* 2009). The high expression of KCC2 in mature CNS determines a decrease of intracellular chloride ion concentration, resulting in a developmental shift in GABA action from depolarization to hyperpolarization. Previous studies on CGNs grown *in vitro* have shown that GABA induced depolarizing responses in immature neurons and E_{rev} of GABA currents negatively shifted between 3 DIV and 8 DIV (Borodinsky *et al.* 2003). KCC2 has been observed to be timely regulated in CGNs *in vivo* during the postnatal development of the mouse cerebellum. The KCC2 expression has been found low in granule cell precursors and migrating granule cells at postnatal day 3 (P3), then the amount of KCC2 increases progressively through P5, reaching its maximum at P21 (Takayama and Inoue 2006). The study of Takayama *et al.*, suggested that, early in cerebellum development, GABA might act as an excitatory transmitter on the immature granule cells, with low KCC2 level, that are migrating from the external molecular layer, passing through the Purkinje cell layer, and entering the internal granular layer. On the contrary, late during the maturation process, the gradual increase of KCC2 expression may induce the developmental shift, from depolarization to hyperpolarization, thus GABA may become an inhibitory transmitter when GABAergic synapses between granule cells and Golgi cells are formed (Takayama and Inoue 2006). As described in others

Fig. 7 miR-92 inhibition produces a hyperpolarizing effect in CGNs. (a) Representative current recordings elicited by 10 μM GABA at different holding potential recorded in pLSyn and pLSyn-miR-92 sponge CGNs in the gramicidin-perforated patch condition. (b) Current-voltage relationship of the GABA-induced currents from the neurons shown in (a). (c) Scatter plot of E_{rev} for pLSyn and pLSyn-miR-92 sponge cells. The mean values for E_{rev} (bar) were -51.6 ± 11.2 mV ($n = 10$) for pLSyn neurons and -61.3 ± 6.9 mV ($n = 9$) for pLSyn-miR-92 sponge cells (t-test; $p < 0.04$). (d) Scatter plot of intracellular chloride $[Cl^-]_i$. The $[Cl^-]_i$ mean values (bar) for pLSyn and pLSyn-miR-92 sponge were significantly different (21.6 ± 9.7 mM, $n = 10$ and 14.1 ± 3.7 mM, $n = 9$, respectively; t-test $p < 0.05$). (e) Means and SD of the driving force of pLSyn ($n = 10$) and pLSyn-miR-92 sponge ($n = 9$) neurons at 6 DIV. The mean values of pLSyn-miR-92 sponge cells are significantly different compared to pLSyn cells (-4.4 ± 6.2 mV, $n = 9$ and 5.5 ± 7.3 mV, $n = 10$, respectively; t-test $p < 0.001$).
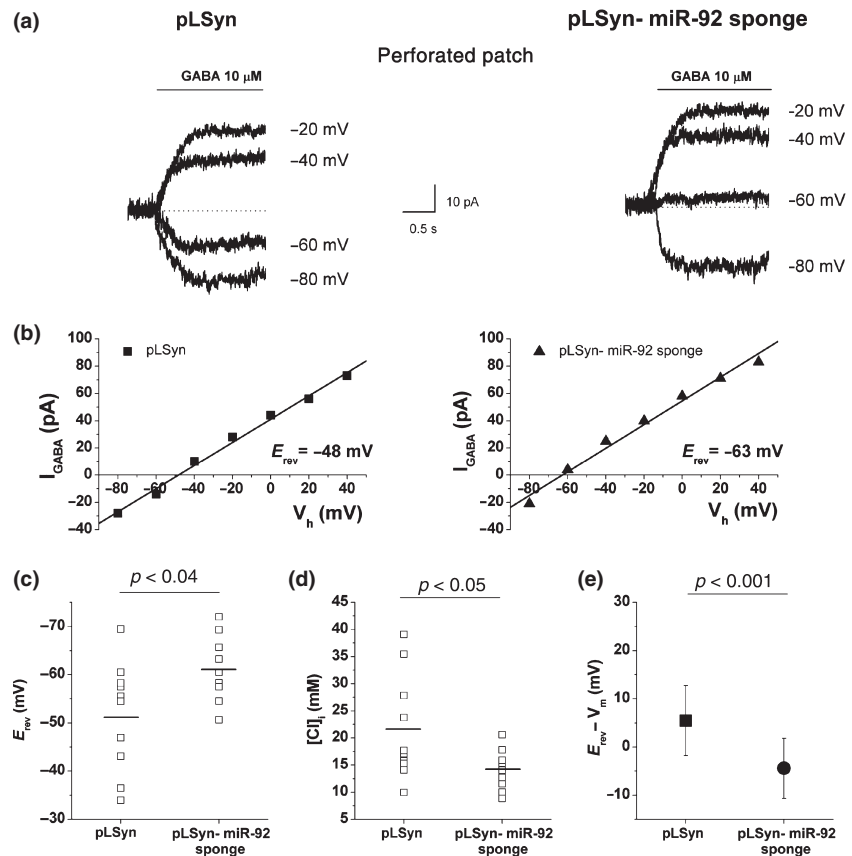
neuronal systems (Cancedda *et al.* 2007; Bortone and Polleux 2009), GABA responses, modulated by KCC2 expression, might play an important role in regulation of CGNs migration and maturation. It seems that the fine-tuning of KCC2 expression during the cerebellar granule maturation might allow the complex events in the cerebellum development to occur. We propose that miR-92 may be involved, by regulating KCC2 abundance during maturation, in determining the gradual shift of GABA from depolarization to hyperpolarization. Consistently with this hypothesis, we found that the over-expression of miR-92 in CGNs at 8 DIV induced a change in reversal potential of GABA-induced Cl(−) currents and this phenotype was reversed by KCC2 re-expression. Moreover inhibition of endogenous miR-92 in CGNs at 6 DIV, leading to a robust KCC2 expression, accelerated the negative shift of GABA reversal potential. In developing neurons intracellular Cl(−) concentration is the result of the combined actions of NKCC1 and KCC2 which respectively accumulates and extrudes intracellular Cl(−) thus establishing the polarity of GABA responses (Blaesse *et al.* 2009). Although NKCC1 may be involved in the establishment of intracellular Cl(−) concentration in CGNs, our data showed that the decrease of intracellular Cl(−) concentration mediated by miR-92 over-expression was reversed by KCC2 re-expression, thus suggesting a significant role of KCC2 in CGNs.

It should be considered that miR-92 such as other microRNAs might act in concert with a transcriptional control to define the fine-tuning regulation of KCC2 expression. Indeed, it has been shown that KCC2 expression is transcriptionally regulated in mouse cerebellum during postnatal development by the transcription factor early growth response 4 (Uvarov *et al.* 2006) In addition recently the REST-dual RE-1 (repressor element-1) interaction was identified as a novel mechanism of KCC2 transcriptional regulation that significantly contributes to the developmental switch in neuronal chloride concentration and GABA action in cortical neurons (Yeo *et al.* 2009). Our findings together with these studies provide a framework to further elucidate the developmental regulation of KCC2 expression and the consequent switch in neuronal chloride concentration.

The regulatory circuit mediated by miR-92 that we have described in the developing cerebellum could be also important in other brain areas, as hippocampus, in which KCC2 expression has been shown to be developmentally regulated (Lu *et al.* 1999). Indeed, preliminary results indicated that, beside CGNs, miR-92 is down-regulated in hippocampal tissue from P2 to P14 (data not shown).

As a final remark, we would like to note that miR-92 is included in miR-17/18a/19/20a/19b1/92a cluster (miR-17-92 cluster) (He *et al.* 2005). In mammals, the miR-17-92 cluster, also called Oncomir-1, was among the first miRNAs to be

validated as showing oncogenic potential (He *et al.* 2005). In the nervous system the up-regulation of miR-17-92 cluster expression has been associated to a subtype of medulloblastoma, a malignant pediatric brain tumor, originating from cerebellar granule neuron precursors (Uziel *et al.* 2009). This evidence may suggest that miR-92, perhaps with the other miRNAs present in the cluster, may play a role not only in the maturation process of post-mitotic CGNs but also in controlling the transition from the proliferative state of CGN precursors to the post-mitotic state of maturing CGNs.

Acknowledgements

References

Akaike N. (1996) Gramicidin perforated patch recording and intracellular chloride activity in excitable cells. *Prog. Biophys. Mol. Biol.* **65**, 251–264.

Ashraf S. I. and Kunes S. (2006) A trace of silence: memory and microRNA at the synapse. *Curr. Opin. Neurobiol.* **16**, 535–539.

Barbato C., Giorgi C., Catalanotto C. and Cogoni C. (2008) Thinking about RNA? MicroRNAs in the brain. *Mamm. Genome* **19**, 541–551.

Bartel D. P. (2004) MicroRNAs: genomics, biogenesis, mechanism, and function. *Cell* **116**, 281–297.

Bartel D. P. (2009) MicroRNAs: target recognition and regulatory functions. *Cell* **136**, 215–233.

Blaesse P., Airaksinen M. S., Rivera C. and Kaila K. (2009) Cation-chloride cotransporters and neuronal function. *Neuron* **61**, 820–838.

Borodinsky L. N., O'Leary D., Neale J. H., Vicini S., Coso O. A. and Fiszman M. L. (2003) GABA-induced neurite outgrowth of cerebellar granule cells is mediated by GABA(A) receptor activation, calcium influx and CaMKII and erk1/2 pathways. *J. Neurochem.* **84**, 1411–1420.

Bortone D. and Polleux F. (2009) KCC2 expression promotes the termination of cortical interneuron migration in a voltage-sensitive calcium-dependent manner. *Neuron.* **62**, 53–71.

Cancedda L., Fiumelli H., Chen K. and Poo M. M. (2007) Excitatory GABA action is essential for morphological maturation of cortical neurons in vivo. *J. Neurosci.* **27**, 5224–5235.

Dull T., Zufferey R., Kelly M., Mandel R. J., Nguyen M., Trono D. and Naldini L. (1998) A third-generation lentivirus vector with a conditional packaging system. *J. Virol.* **72**, 8463–8471.

Ebert M. S., Neilson J. R. and Sharp P. A. (2007) MicroRNA sponges: competitive inhibitors of small RNAs in mammalian cells. *Nat. Methods.* **4**, 721–726.

Gentner B., Schira G., Giustacchini A., Amendola M., Brown B. D., Ponzoni M. and Naldini L. (2009) Stable knockdown of microRNA in vivo by lentiviral vectors. *Nat. Methods.* **6**, 63–66.

Griffiths-Jones S. (2006) miRBase: the microRNA sequence database. *Methods Mol. Biol.* **342**, 129–138.

Grimson A., Farh K. K., Johnston W. K., Garrett-Engele P., Lim L. P. and Bartel D. P. (2007) MicroRNA targeting specificity in mammals: determinants beyond seed pairing. *Mol. Cell* **27**, 91–105.

He L., Thomson J. M., Hemann M. T. *et al.* (2005) A microRNA polycistron as a potential human oncogene. *Nature* **435**, 828–833.

Kissler S., Stern P., Takahashi K., Hunter K., Peterson L. B. and Wicker L. S. (2006) In vivo RNA interference demonstrates a role for Nramp1 in modifying susceptibility to type 1 diabetes. *Nat. Genet.* **38**, 479–483.

Kosik K. S. (2006) The neuronal microRNA system. *Nat. Rev. Neurosci.* **7**, 911–920.

Krek A., Grün D., Poy M. N. *et al.* (2005) Combinatorial microRNA target predictions. *Nat. Genet.* **37**, 495–500.

Kügler S., Meyn L., Holzmüller H., Gerhardt E., Isenmann S., Schultz J. B. and Bähr M. (2001) Neuron-specific expression of therapeutic proteins: evaluation of different cellular promoters in recombinant adenoviral vectors. *Mol. Cell. Neurosci.* **17**, 78–96.

Kyrozis A. and Reichling D. B. (1995) Perforated-patch recording with gramicidin avoids artifactual changes in intracellular chloride concentration. *J. Neurosci. Methods* **57**, 27–35.

Lagos-Quintana M., Rauhut R., Yalcin A., Meyer J., Lendeckel W. and Tuschl T. (2002) Identification of tissue-specific microRNAs from mouse. *Curr. Biol.* **12**, 735–739.

Lewis B. P., Burge C. B. and Bartel D. P. (2005) Conserved seed pairing, often flanked by adenosines, indicates that thousands of human genes are microRNA targets. *Cell* **120**, 15–20.

Lu J., Karadsheh M. and Delpire E. (1999) Developmental regulation of the neuronal-specific isoform of K-Cl (-) cotransporter KCC2 in postnatal rat brains. *J. Neurobiol.* **39**, 558–568.

Mikawa S., Wang C., Shu F., Wang T., Fukuda A. and Sato K. (2002) Developmental changes in KCC1, KCC2 and NKCC1 mRNAs in the rat cerebellum. *Brain Res. Dev. Brain Res.* **136**, 93–100.

Nakanishi S. and Okazawa M. (2006) Membrane potential-regulated Ca2+ signalling in development and maturation of mammalian cerebellar granule cells. *J. Physiol.* **575**, 389–395.

Ruberti F. and Dotti C. G. (2000) Involvement of the proximal C terminus of the AMPA receptor subunit GluR1 in dendritic sorting. *J. Neurosci.* **20**, RC78.

Schratt G. (2009) Fine-tuning neural gene expression with microRNAs. *Curr. Opin. Neurobiol.* **19**, 213–219.

Takayama C. and Inoue Y. (2006) Developmental localization of potassium chloride co-transporter 2 in granule cells of the early postnatal mouse cerebellum with special reference to the synapse formation. *Neuroscience* **143**, 757–767.

Uvarov P., Ludwig A., Markkanen M., Rivera C. and Airaksinen M. S. (2006) Upregulation of the neuron-specific K+/Cl- cotransporter expression by transcription factor early growth response 4. *J. Neurosci.* **26**, 13463–13473.

Uziel T., Karginov F. V., Xie S. *et al.* (2009) The miR-17~92 cluster collaborates with the Sonic Hedgehog pathway in medulloblastoma. *Proc. Natl Acad. Sci. USA* **106**, 2812–2817.

Wang X. and El Naqa I. M. (2008) Prediction of both conserved and nonconserved microRNA targets in animals. *Bioinformatics* **24**, 325–332.

Yekta S., Shih I. H. and Bartel D. P. (2004) MicroRNA-directed cleavage of HOXB8 mRNA. *Science* **304**, 594–596.

Yeo M., Berglund K., Augustine G. and Liedtke W. (2009) Novel repression of Kcc2 transcription by REST-RE-1 controls developmental switch in neuronal chloride. *J. Neurosci.* **29**, 14652–14662.